

University of Mississippi

eGrove

Honors Theses

Honors College (Sally McDonnell Barksdale
Honors College)

Spring 5-9-2020

Isolation, Identification, and Investigation of a Novel Bioactive Furanocoumarin from Leaves of *Amyris elemifera*

Amy K. Bracken

Follow this and additional works at: https://egrove.olemiss.edu/hon_thesis



Part of the [Medicinal-Pharmaceutical Chemistry Commons](#), and the [Other Chemistry Commons](#)

Recommended Citation

Bracken, Amy K., "Isolation, Identification, and Investigation of a Novel Bioactive Furanocoumarin from Leaves of *Amyris elemifera*" (2020). *Honors Theses*. 1324.

https://egrove.olemiss.edu/hon_thesis/1324

This Undergraduate Thesis is brought to you for free and open access by the Honors College (Sally McDonnell Barksdale Honors College) at eGrove. It has been accepted for inclusion in Honors Theses by an authorized administrator of eGrove. For more information, please contact egrove@olemiss.edu.

ISOLATION, IDENTIFICATION, AND INVESTIGATION OF A NOVEL
BIOACTIVE FURANOCOUMARIN FROM LEAVES OF AMYRIS ELEMIFERA


By Amy Katherine Bracken

A thesis submitted to the faculty of The University of Mississippi in partial
fulfillment of the requirements of the Sally McDonnell Barksdale Honors College

Oxford

May 2020

Approved By:

A handwritten signature in cursive script, appearing to read "Susan Pedigo", written over a horizontal line.

Advisor: Dr. Susan Pedigo

A handwritten signature in cursive script, appearing to read "Kumudini Meepagala", written over a horizontal line.

Reader: Dr. Kumudini Meepagala

A handwritten signature in cursive script, appearing to read "Nathan Hammer", written over a horizontal line.

Reader: Dr. Nathan Hammer

A handwritten signature in cursive script, appearing to read "Gerald Rowland", written over a horizontal line.

Reader: Dr. Gerald Rowland

©2020

Amy Katherine Bracken

ALL RIGHTS RESERVED

ACKNOWLEDGEMENTS

First, I would like to thank the United States Department of Agriculture Natural Products Utilization Research Unit for permitting me to use all of the equipment and materials necessary to complete this project. Furthermore, I would like to express my gratitude to Dr. Kumudini Meepagala, who has graciously allowed me to work in her lab for the past few years. She has been an amazing mentor and cheerleader, and I will always be grateful for my time spent working with her. Additionally, I would like to thank Linda Robertson, Bob Johnson, Caleb Anderson, and the other staff members at the National Center for Natural Products who helped with some of the techniques used throughout this project. Furthermore, I must thank the Sally McDonnell Barksdale Honors College for granting me the necessary funds to present some of this research at an ACS National Conference. I would also like to thank my professors in the Department of Chemistry for cultivating my love of the subject and encouraging me in my research endeavors. Lastly, I would like to thank my friends and family for all of their support and love in my time at the University of Mississippi, which has made all the difference in my experience here.

ABSTRACT

Plants produce biologically active compounds that humans have utilized for many agricultural applications. *Amyris elemifera* was investigated due to the known bioactivity of its family, Rutaceae, and its use in medicines in tribes of the Bahamas. Biotage® and TLC guided fractionation of the EtOAc, hexane, and MeOH extracts of the leaves of *Amyris elemifera* yielded bioactive compounds. Most significantly, a novel furanocoumarin, 8-(3-methylbut-2-enyloxy)-marmesin acetate (**1**), and its analog 8-(3-methylbut-2-enyloxy)-marmesin (**2**), were isolated. The structures were identified via NMR and X-ray crystallography techniques; the X-ray crystal structure for **1** was reported for the first time, and the data confirmed an absolute configuration of S at the chiral C-2' for both compounds, which had not been reported previously for **2**. Both were tested for activity against monocots, dicots, and fungi. The compounds hindered growth of *Lactuca sativa* (lettuce) and *Agrostis stolonifera*. A *Lemna paucicostata* phytotoxicity bioassay reported IC₅₀ values for **1** and **2** as 26.2µM and 102µM respectively, and **1** showed antifungal activity against *Colletotrichum fragariae* in a TLC bioautography. The mechanism of phytotoxicity was shown to be membrane function related from the results of a cellular leakage assay. In a comparison of bioactivity between **1** and limonene, **1** unexpectedly showed more inhibition on fungal and bacterial species tested.

TABLE OF CONTENTS

List of Figures.	vi
List of Abbreviations.	vii
Introduction.	1
Experimental Methods.	9
Results and Discussion.	19
I. Identification and Analysis of 1 and 2.	19
II. Bioactivity of Isolated Compounds.	27
III. Comparison of 1 to (S)-Limonene.	35
Conclusion.	39
References.	41
Appendix.	44

LIST OF FIGURES

Figure 1	The structure of (S)-Limonene.	3
Figure 2	The reaction of pectin methyl esterase.	5
Figure 3	The structure of psoralen.	5
Figure 4	Psoralen's mechanism of action against DNA transcription.	6
Figure 5	The structure of 8-methoxypsoralen.	7
Figure 6	TLC results of fractions 20 and 21.	19
Figure 7	Structure of 8-(3-methylbut-2-enyloxy)-marmesin acetate (1).	20
Figure 8	¹ HNMR spectrum of 1	21
Figure 9	DQ-COSY spectrum of 1	22
Figure 10	COSY correlations between hydrogens in 1	23
Figure 11	The structure of 8-(3-methylbut-2-enyloxy)-marmesin (2).	24
Figure 12	HPLC chromatogram of crude EtOAc extract and pure 1	25
Figure 13	Calibration curve of fraction 20-21 from HPLC.	25
Figure 14	X-Ray crystallographic data structure of 1	26
Figure 15	Results from the <i>L. pausicostata</i> assay of 1	29
Figure 16	Results from the <i>L. pausicostata</i> assay of 2	30
Figure 17	Cellular membrane leakage results of 1	32
Figure 18	Anthracnose crown rot effects on strawberries.	33
Figure 19	TLC bioautography results of 1	34
Figure 20	TLC bioautography results of (S)-Limonene.	37

LIST OF ABBREVIATIONS

TLC	Thin Layer Chromatography
PME	Pectin Methyl Esterase
EtOAc	Ethyl Acetate
DCM	Dichloromethane
MeOH	Methanol
ACN	Acetonitrile
PAR	Photosynthetically Active Radiation
NMR	Nuclear Magnetic Resonance
MS	Mass Spectrometry
VRE	Vancomycin-resistant enterococci
MRSA	Methicillin-resistant <i>Staphylococcus aureus</i>
BRS	Broad Signal (in NMR spectra)

Introduction

As concerns about the health of the global environment rise, synthetic chemicals used in agriculture as herbicides, pesticides, fungicides, etc. have come under scrutiny regarding their environmental impact and have caused the implementation of stricter legislation governing which synthetic compounds can be utilized ^[1]. Synthetic products typically have more environmental influences due to the presence of unnatural carbon structures and halogens, which have significantly longer lifetimes and reactivity than the majority carbon, oxygen, and nitrogen rich structures of natural products. These long environmental lifetimes increase the potentially harmful effects on crops upon degradation, as the decomposed by-products usually retain toxicity ^[1]. Furthermore, the continued overuse of synthetic agricultural enhancers has led to an increased issue of resistant species, indicating that a major change is necessary in the mechanism of crop defense ^[2]. Natural products, or those produced by living organisms (*in vivo*), therefore seem to be the answer to the question of maintaining sustainable agriculture and fighting off species that would harm crops.

Utilization of natural products from plants often focuses on their secondary metabolites, which are more unique among different families/genera/species/etc. and are usually active specifically against other plants to enhance the success of the organism that produces them ^[3]. Primary metabolites in plants are common

amongst different classifications and are vital in any plants' survival and proper growth, and are therefore less helpful in producing targeted herbicides, pesticides, fungicides, etc. because of the biological usefulness of such compounds [3]. Plant secondary metabolites are often phytotoxic, antifungal, and insecticidal due to the need for survival mechanisms against competitive organisms in their respective environments. These fundamental characteristics of bioactive plant secondary metabolites guided the investigation outlined in this paper, of which the fundamental purpose was to isolate secondary metabolites that could potentially be used as defenses against crop inhibitors in agricultural applications.

Plants with a plethora of secondary metabolites are often focused on in the search for crop defenses, since their range of active compounds is vast and holds many opportunities for finding a significant constituent. A family of plants that is famous for its secondary metabolite diversity is the Rutaceae family, most notably consisting of the Citrus genus [4]. According to Nebo *et al.*, the classes of compounds most likely to be useful in agricultural protection are alkaloids, limonoids, terpenoids, coumarins, and flavonoids—all of which have been commonly observed in members of the Rutaceae family [4]. One member of the Rutaceae family, *Amyris elemifera*, has been used to treat several ailments by several Bahamian ethnic groups on Abaco island [5]. According to Setzer *et al.* its healing effects on wounds, influenza, and general illnesses warranted investigation into the plant's essential oils, revealing that the major constituent of the oil was limonene (45%), an extremely common monoterpene amongst

Rutaceae plants [5]. Monoterpenes are known to be very promising in agricultural defense applications, with thorough research over the extent of their herbicidal, fungicidal, insecticidal, and bactericidal activity [6]. Limonene has been extensively studied due to its healing properties in human health applications—it has been shown to completely dissolve cholesterol (i.e. in gall stones), alleviate heartburn, activate carcinogen-metabolizing enzymes, and inhibit tumor cell proliferation to an extent [7]. The structure of (S)-limonene is shown in **Figure 1**; since the S/D enantiomer is more bioactive than the R/L stereoisomer, the former was focused on for the purposes of this investigation [8]. This thesis included limonene in the investigation to perform a bioactivity comparison between the well-known essential oil component and the new furanocoumarin.

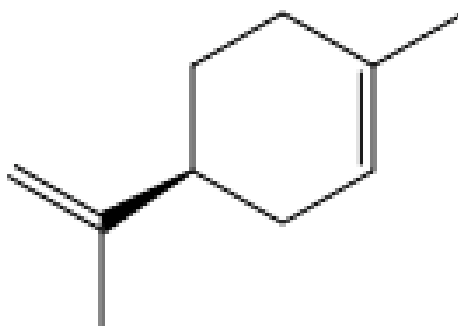


Figure 1. The structure of (S)-Limonene.

Marei *et al.* outlines two potential mechanisms for limonene's mechanism of action against fungi: inhibitory effects on cellulase and pectin methyl esterase (PME) [6]. Cellulase is used by pathogenic fungi to degrade the cell walls of its target, so inhibition of the enzyme eventually prevents pathogenesis from occurring [6]. PME regulates the methyl esterification of pectins, which are

essential polysaccharides embedded in the cell walls of most terrestrial plants [6]. Normal function of PME is necessary for maintaining a cells' pH environment as well as significant processes in plant growth, like stem and root elongation [9]. The demethylesterification reaction of PME on pectin polymers is shown in **Figure 2** [10]. Furthermore, PME needs to be functioning properly in order to release MeOH (**Figure 2**) and oligogalacturonides (OG's) that signal to the cell a pathogenic attack has occurred and immune responses should be activated [11]. Therefore, pathogens and compounds that affect PME must inhibit its proper function and prevent MeOH and OG's from being secreted in order to hinder the target's ability to defend itself from the attack. Generally, it is well substantiated that monoterpenes alter structure and/or function in cellular membranes due to their lipophilic characteristics—this could refer to either changing membrane permeability or interrupting cellular processes that take place across the membrane of the pathogen or victim (i.e. respiration) [6].

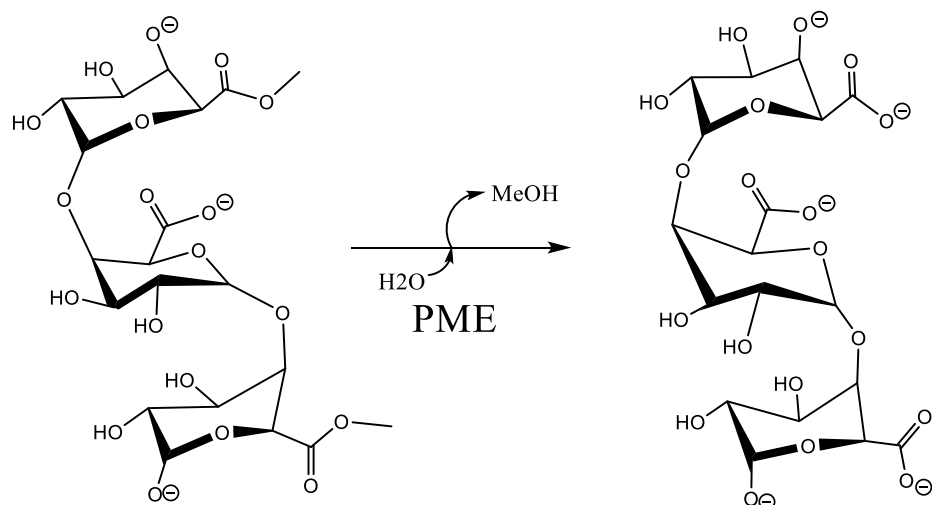


Figure 2. The reaction of Pectin methyl esterase (PME) on a general pectin polymer. Adapted from Reference #10: Salas-Tovar, Jesús A., et al. “Analytical Methods for Pectin Methyl esterase Activity Determination: A Review.” *Food Analytical Methods*, vol. 10, no. 11, 2017, pp. 3634–3646., doi:10.1007/s12161-017-0934-y.

Additionally, furanocoumarins, like the novel compound of interest in this investigation, have a general proposed mechanism for their bioactivity—though it is too complex to be entirely understood as of yet. Most of the studied furanocoumarins are derivatives of psoralen (**Figure 3**), so the mechanism discussed may be slightly different to the newly isolated species, though extreme discrepancies are unlikely [12].

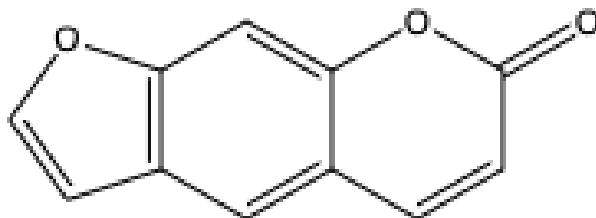


Figure 3. The structure of psoralen, one of the most common furanocoumarins studied.

Briefly, furanocoumarins undergo a photoreaction with DNA to alter the transcription capabilities of cells and ultimately induce cell death [12]. The three general steps of the mechanism include an initial weak intermolecular interaction between pyrimidine bases and the furanocoumarin, formation of the pyrimidine-furanocoumarin product, and then an additional pyrimidine addition to the remaining alkene site of the furanocoumarin [12]. These steps are summarized in **Figure 4**, showing a reaction between psoralen and the nitrogenous base thymine [12].

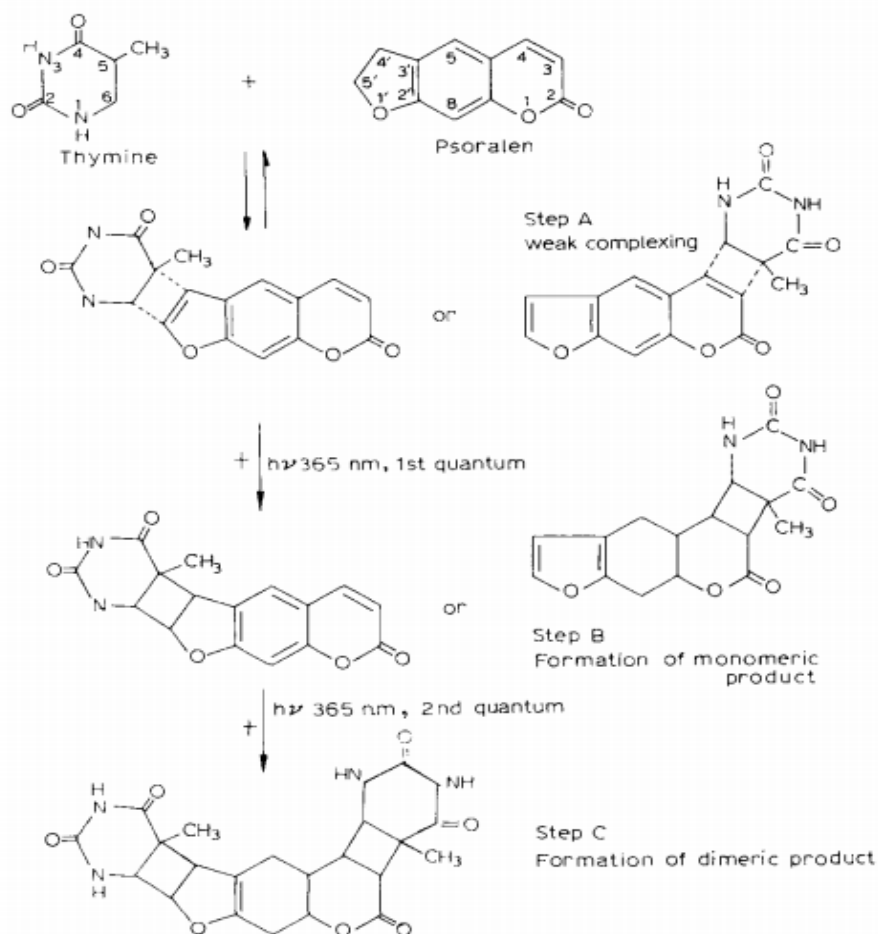


Figure 4. The mechanism of action that psoralen, undergoes in order to alter DNA transcription and produce the desired effect in the victim organism. Taken with permission from Reference 12: Scott, Barry R., et al. "Molecular and Genetic Basis of Furocoumarin Reactions." *Mutation Research/Reviews in Genetic Toxicology*, vol. 39, no. 1, 1976, pp. 29–74., doi:10.1016/0165-1110(76)90012-9.

It is important to note that only photoactive furanocoumarins exhibit the full binding with pyrimidines, nucleosides, and nucleotides (step 2) and the formation of the dimer only occurs if the 4',5 double bond of the furanocoumarin is the first to react with the substrate, due to the remaining ability of the 3,4 double bond to absorb UV energy and create the subsequent dimeric product [12]. The scope of this investigation did not include a thorough studying of the novel furanocoumarin's photoactivity, though it is structurally similar to 8-methoxypsoralen (**Figure 5**), which is very photoactive and typically has extensive effects on DNA transcription [12].

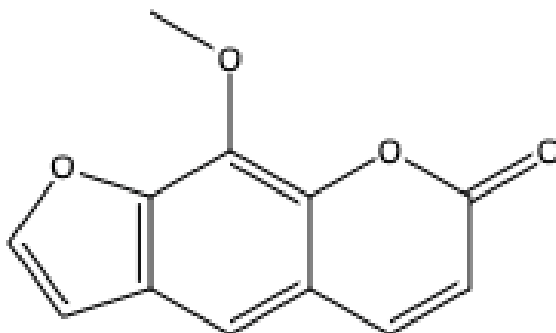


Figure 5. The structure of 8-methoxypsoralen, another highly active furanocoumarin.

Analogs are structurally similar compounds, and synthetic analogs are often used in lieu of the natural product to alleviate the tedious process of isolating the compound. This thesis investigated a previously studied analog of the new furanocoumarin, 8-(3-methylbut-2-enyloxy)-marmesin, to compare the bioactivities and properties of the two analogs and determine which would be most useful in agricultural applications. Both analogs were isolated naturally from the plant, but the marmesin acetate analog was significantly more abundant

in the extracts; consequently, the hydroxy analog was synthetically derived in a reaction from the acetate to make enough of the 8-(3-methylbut-2-enyloxy)-marmesin for a thorough investigation. The methods described below outline the isolation and structure elucidation of both analogs, as well as the inquiry into the bioactivity of both compounds using various bioassays.

Experimental Methods

Instrumentation and General Methods.

All solvents used in the experiments were reagent grade and not further purified. Thin-Layer chromatography (TLC) was performed on 250 μ m silica gel plates with a fluorescent indicator (Analtech, Newark, DE). The compounds on the TLC plates were visualized using UV light at 254nm and 365nm, *para*-anisaldehyde spray reagent, Dragendorff spray reagent (Sigma-Aldrich, St. Louis, MO), and an Iodine vapor tank. Fractionation through column chromatography was carried out using a Biotage IsoleraTM Flash Chromatography system equipped with a dual-wavelength (254nm and 280nm) detector using silica gel SNAP Ultra columns (particle size 40-65 μ m) in varying ethyl acetate (EtOAc) and hexane gradients (Biotage Inc., Charlottesville, VA). Bruker NMR spectrometers (Billerica, MA) were used to record the H¹ and C¹³ NMR spectra and operated at 400MHz and 100MHz for H¹NMR and C¹³NMR respectively. High resolution mass spectra were recorded on a Jeol ACCU TOF 4G LC mass spectrometer (Jeol, Tokyo, Japan) with a DART ion source (IonSense DART controller, Sangus, MA). All relevant experimental spectra are found in either the **Results and Discussion** or **Appendix** section of this thesis. The optical rotations were obtained using an Autopol IV Automatic Polarimeter model 589-546 (Rudolph Research Analytical, Hackettstown, NJ). An Optimelt

melting point instrument (Stanford Research System, Sunnyvale, CA) was used to measure melting points.

Plant Material and Extraction.

The studied leaves of *Amyris elemifera* were collected in Miami-Dade County, FL, USA in April 2009. Dr. Charles Burandt of the University of Mississippi School of Pharmacy identified the leaves, and a voucher specimen has been deposited in the University of Mississippi herbarium BUR 280703. The leaves were ground, air-dried, and stored in plastic bottles at 25°C until they were extracted. 500g of the leaves were extracted with 2 Liters of hexane, EtOAc, and MeOH twice each at room temperature, yielding 10g, 49g, and 64g of the extracts respectively. Each extract was tested for phytotoxicity, but only the EtOAc extract tested positively for phytotoxic activity. TLC of the EtOAc extract showed a major UV active constituent and several minor components.

Isolation and General Analysis of Compounds.

Part of the EtOAc extract (29g) was loaded onto a 340g SNAP Ultra Biotage column and fractionated using an EtOAc in hexane gradient (0-100%) elution. The Biotage instrument is used to run automated column chromatography, and it collects fractions based upon UV activity that it detects. As a compound elutes from the column (known by a sudden change in UV absorption), the sample is collected into test tubes until the detector senses a return to the base line UV absorption of the column and solvents. This allows for easy separation of compounds in complex and large samples, like plant extracts. TLC was used to

analyze the fractions, and those that were similar were combined according to the TLC results to yield a total of 28 fractions. The TLC technique relies on the fact that compounds and solvents with similar polarities are more likely to bind together than those with opposing polarities. Briefly, a sample is applied to a stationary phase (a silica plate, in this investigation) and the plate is placed into a solvent. The solvent runs up the stationary phase, and depending on its polarity, will separate certain compounds based on how well the compounds' polarity matches the solvent's. The final solvent composition (mix of two solvents) is chosen to optimize the separation of the constituents on the plate, which is usually determined through several trials of typical solvent mixtures (i.e. 50% EtOAc/Hex, 10% IPA/Hex, etc.) that have success with natural products' separation in our lab. Comparing the TLC results of compounds in the same solvent will show whether or not the identity of the compounds could be identical; the compounds will move exactly the same distance up the plate, and will look the same in the visualization technique used on the plate, if they are the same. All fractions combined after TLC analysis were tested for phytotoxicity, and fractions 20 and 21 showed a major compound with high phytotoxicity and antifungal activity. These two fractions were combined and further purified using a 50g SNAP Ultra Biotage column with a 20-60% EtOAc in hexane gradient elution. Utilizing a gradient elution for collection of the compounds (versus isocratic runs for the purely analytical TLC's) allows the increasing concentration of polar solvent (EtOAc in this case) to eventually out-compete the polar-polar interactions of the components and the polar silica stationary phase at a high

enough concentration. The major component was crystallized using EtOAc, dichloromethane (DCM), and hexane, which yielded white crystals that were determined to be 8-(3-methylbut-2-enyloxy)-marmesin acetate (**1**). Fraction 24 (56mg) of the EtOAc extract was run through a Florisil® column (8cm x 1.8cm) to remove chlorophyll using a 30% EtOAc/Hexane mobile phase and collecting fractions manually. Chlorophyll is highly UV active, and therefore interferes with the ability to focus on compounds of interest. Florisil® (magnesium silicate) is very successful as an adsorbent for lipids like chlorophyll, allowing for them to be separated from samples when they are run through a column packed with Florisil® [13]. The resulting fractions without chlorophyll were run on using Biotage flash chromatography with a 10g silica gel column and 30-80% EtOAc/Hexane gradient. From the Biotage fractionation, 38mg of 8-(3-methylbut-2-enyloxy)-marmesin (**2**), a colorless gum after evaporation of all solvent, was isolated.

Quantification of 1 in the EtOAc Extract Using HPLC.

Liquid chromatography was performed on an Agilent 1260 Infinity HPLC system with quaternary pump and diode array detector. A LUNA C-18 100A column (250 x 4.6mm, Phenomenex, USA) with silica guard column (10 x 3 mm) was used in the method run at 25°C. This column utilizes an 18-carbon chain as the stationary phase (therefore is reverse phase, since C-18 is hydrophobic), allowing non-polar compounds to stick to the non-polar column and polar compounds to elute more quickly. The mobile phase was also polar, at a 5-95% Acetonitrile (ACN) in 0.1% formic acid/water gradient run over 20 minutes at a

flow rate of 1.0 mL/min and injection volume of 5 μ L. Two UV wavelengths, 254nm and 280nm, were used to monitor the signals on the chromatogram. A standard calibration curve ($R^2 = 1.0$) was constructed of pure **1** at concentrations 0.0312, 0.0625, 0.125, 0.25, 0.5, and 1 mg/mL in DCM. The crude EtOAc extract at concentrations 0.5 and 1mg/mL were used for the quantification of **1** using the curve.

X-Ray Crystallography of 1.

Data were collected by Dr. Frank R. Fronczek (Louisiana State University) at 90 K with $\text{CuK}\alpha$ ($\lambda = 1.54184 \text{ \AA}$) radiation using a Bruker KappaAPEX II DUO diffractometer with microfocus source. The absolute configuration of **1** was found from Flack parameter $x = 0.05$ (3) based on 1446 quotients. The orthorhombic space group of **1** was determined to be $P2_12_12_1$. Experimental data showed $a = 7.5977$ (12) \AA , $b = 12.622$ (2) \AA , $c = 19.483$ (3) \AA , $V = 1868.5$ (5) \AA^3 , $Z = 4$, and $\mu = 0.80 \text{ mm}^{-1}$. Refinement yielded an R value of 0.028 using 3467 reflections, $\theta = 3.5$ -69.3 $^\circ$, and 250 parameters. A subsequent, higher resolution refinement was done based on data up to $\theta_{\text{max}} = 39.3^\circ$ using $\text{MoK}\alpha$ radiation. The results from both refinements have been submitted to the Cambridge Crystallographic Data Centre with the deposition numbers CCDC 1866085 and 1866086.

Base Hydrolysis of 1 to Yield 2.

After isolating **1**, 200mg of it was dissolved in 10mL of MeOH and added to 20mL of 10% aqueous KOH. The solution was stirred at room temperature for 4 hours. Then, the mixture was diluted with 50mL water, acidified with 1M HCl,

extracted twice with 75mL DCM, and washed with 50mL water and 50mL saturated brine. The resulting solution was dried over anhydrous Na₂SO₄ before evaporating the solvent. The product, a viscous and colorless gum, was purified using Biotage flash chromatography—a 10g silica gel column with 80% EtOAc/Hexane mobile phase—to obtain the final product of pure **2**, whose identity was confirmed through NMR and optical rotation data.

Phytotoxicity Bioassay.

Extracts and purified components were submitted to this bioassay, which measures samples' effect on seed germination and growth against *Lactuca sativa* (lettuce, a dicot) and *Agrostis stolonifera* (creeping bentgrass, a monocot) in a procedure developed by Dayan *et al* ^[14]. Seeds of both species are put in 24-well plates, and samples are dissolved in a 10% acetone/DI water mixture before addition of 250µL of the sample/transfer solvent solution to the wells. Control wells were treated with the 10% acetone/DI water mixture only. Acetone was used as the transfer solvent due to its well-proven lack of physical or chemical effect on the types of compounds normally tested in this assay ^[14]. Plates were sealed and incubated under continuous light conditions at 26°C and 120 µmol s⁻¹ m⁻² average photosynthetically active radiation (PAR). After 7 days (*L. sativa*) and 10 days (*A. stolonifera*) of incubation, germination and growth was ranked qualitatively on a scale of 0-5; 0 corresponds to no effect/no difference between the control and sample, while a rank of 5 indicates total inhibition of growth by the sample.

***Lemna paucicostata* Bioassay.**

The purified compounds were analyzed against *L. paucicostata* to quantitatively determine phytotoxic activity of the analogs, which is determined by their effect on leaf growth and coloration. In non-pyrogenic, polystyrene sterile 6-well plates, 4950 μ L of Hoagland media (general purpose, nutrient rich media supporting a wide variety of plants) and 50 μ L of the sample (dissolved in an appropriate solvent) were mixed before adding two 3-frond (leaf) plants of *L. paucicostata* of the same approximate age and size to each well. The plates were incubated for 7 days at 26°C and 120 μ mol s⁻¹ m⁻² average PAR. Graphic templates of the plates were used for LemnaTec image analysis (LemnaTec, Würselen, Germany), with measurements taken on day 0, 7, and some intermittent days in between. The plates were placed into the LemnaTec device, and the instrument provided automated leaf area and chlorophyll fluorescence data [15]. Measurements of frond number, total frond area, and color (indicating chlorotic or necrotic presence) were taken. The comparison of leaf area and coloration between the treated and control plants yields the degree of phytotoxicity of the compounds. Each experiment was performed in triplicate.

Cellular Leakage Test.

Compounds were analyzed with this test to determine if the toxicity included a membrane leakage mechanism of action, according to a modified method created by Duke and Kenyon [16]. In this assay, the amount of endogenous cellular electrolytes that leaked from the treated plant was measured to examine

membrane function. *Cucumis sativus* seeds were grown in a Conviron growth chamber for 6 days at 26°C and 173 $\mu\text{mol s}^{-1}\text{m}^{-2}$ PAR. From *C. sativus* leaves, fifty disks with diameter 4mm were cut and placed in Petri dishes (6mm diameter) along with 5mL of 1mM 2-(4-morpholino) ethane sulfonic acid (MES) buffer that was 2% sucrose by weight. The pH of the solution was altered to 6.5 using 1M NaOH. Samples were dissolved in acetone and added to the Petri dishes at concentrations of 10, 100, and 1000 μM . After exposure to the test chemical, electrical conductivity readings were taken with a dip cell at 25°C and at times 0, 1, 2, 4, 6, and 8 hours after exposure. All Petri dishes were then covered with aluminum foil and left for 18 hours after the initial introduction of the sample, and then the conductivities were again recorded at the previously mentioned time intervals. Then, after placing the dishes in 200 $\mu\text{mol s}^{-1}\text{m}^{-2}$ PAR light, conductivity was again measured at 0, 2, 4, 6, and 8 hours. Many phytotoxic compounds have light-dependent (or light-intensified) electrolyte leakage, so this portion of the assay determines how light affects the efficacy of the phytotoxic samples^[16]. The experiment was performed in triplicate before plotting the averaged percent conductivity change against the time after exposure to the test sample. Cucumber leaf disks boiled in MES buffer for 8 minutes were used to measure a maximum potential membrane leakage of the solution.

Bioautography Against *Colletotrichum fragariae*.

A culture of *C. fragariae* was acquired from Barbara J. Smith, USDA ARS in Poplarville, MS and was held at USDA ARS in University, MS until used. The fungus was grown on potato dextrose agar (PDA, Difco, Detroit, MI) and

incubated under $55 \mu\text{mol s}^{-1}\text{m}^{-2}$ light at 24°C with a 12-hour photocycle. Conidia were extracted and collected according to the procedure established by Wedge et al. [17]. After running the sample compounds and extracts on silica gel TLC plates with varying solvent systems (mostly EtOAc and hexane mixtures), the plates were allowed to dry before they were sprayed with a suspension of the conidia at a concentration of 10^6 spores/mL. The spores on the plates were set to incubate for 4 days in an enclosed, transparent box at 26°C under fluorescent lighting. Areas on the TLC plate with no spore growth indicated the presence of antifungal constituents.

Antimicrobial Bioassay.

Both **1** and (S)-Limonene were tested for antimicrobial activity against *Candida albicans*, *Aspergillus fumigatus*, *Cryptococcus neformans*, MRSA, *E. coli*, *Pseudomonas aeruginosa*, *Klebsiella pneumoniae*, and vancomycin-resistant enterococci (VRE) in a 96-well microplate bioassay. Dissolved compounds were pipetted ($10\mu\text{L}$ per well) into sterile, separate polystyrene microplate wells (Corning Costar Corp., Acton, MA). All solvent was evaporated, then $200\mu\text{L}$ of 0.5 MacFarland bacterial culture was added to each well. Using a VWR Model 2005 incubator (Sheldon Manufacturing, Inc., Cornelius, OR), the microplates were incubated at 29°C . Control wells (positive and negative), in which no test analyte was added, were included for each species. In the preliminary assay, both analytes were dissolved in 100% MeOH so that the final concentration of analyte was $50\mu\text{g/mL}$. In the first assay, which was performed in duplicate, the percent inhibitions of each species by the analytes were compared to the positive

control ciprofloxacin; analytes with greater than 50% inhibition continued to the second assay. In the secondary test, the analytes were tested at 20, 4, and 0.8µg/mL. The 50% inhibition concentration, IC₅₀, was determined for each species in the secondary assay. This assay was performed by Marsha Wright at the National Center for Natural Products Research in the Thad Cochran Research Center.

Results and Discussion

I. Isolation, Identification, and Analysis of 1 and 2.

After performing the separation techniques previously mentioned on the EtOAc plant extract, the TLC of fractions 20 and 21 shows that they shared the major bioactive component, as well as some minor components (**Figure 6**).

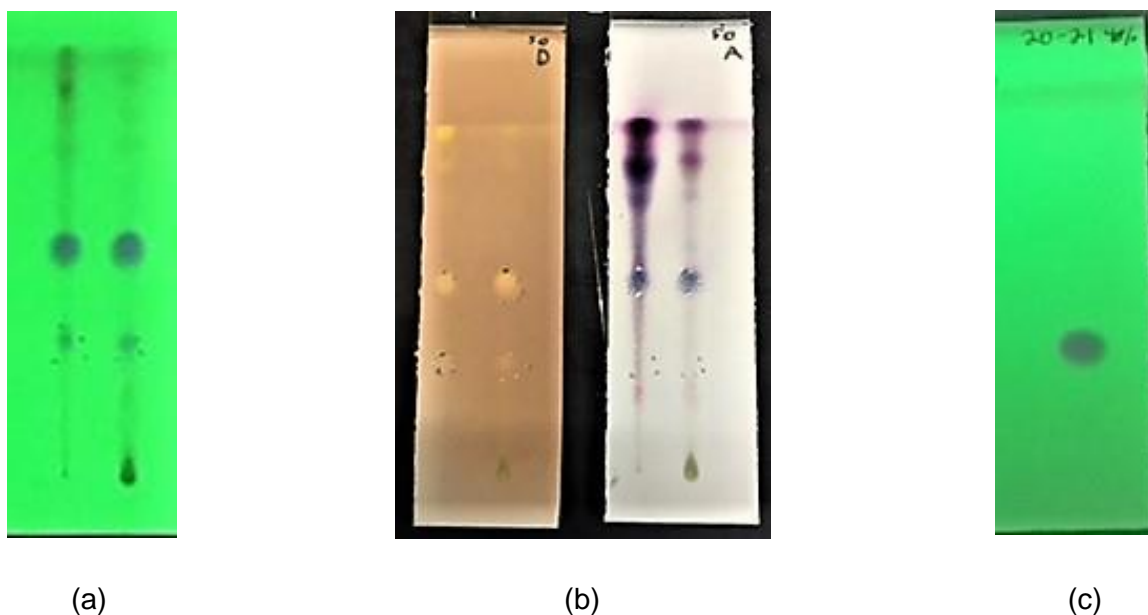


Figure 6. The TLC profiles of fractions 20 (left spot) and 21 (right spot) visualized with (a) 254nm UV light and (b) Dragendorff spray reagent (left) and *p*-anisaldehyde spray reagent (right) after running the plates in a 50% EtOAc/hexane solvent system. Also, the TLC profile of the purified **1** (c), visualized with 254nm UV light after running the plate in a 40% EtOAc/hexane solvent system.

The major component in **Figure 6c** was re-crystallized to produce white crystals that were determined to be 8-(3-methylbut-2-enyloxy)-marmesin acetate (**1**).

Nuclear Magnetic Resonance (NMR) spectra and mass spectra (MS) were analyzed in order to determine the structure of **1** after its isolation into pure crystals (**Figure 7**), which were dissolved in chloroform to collect NMR data and DCM to collect MS data, respectively.

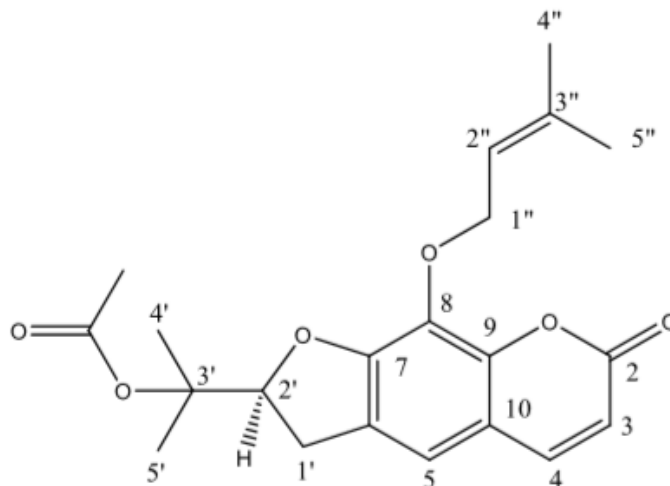


Figure 7. The determined structure of **1**, the novel furanocoumarin.

Figure 8 shows the data produced by the proton NMR ($^1\text{H NMR}$), which gives peaks based upon the chemical environment of hydrogens. The hydrogen that causes a certain peak gives a signal with information about hydrogens on an adjacent carbon to the carbon attached to the hydrogen producing the peak. The data obtained from **Figure 8** yielded the following results: $^1\text{H NMR}$ (400 MHz, CDCl_3) δ 1.53 (s, 3H, 5'- CH_3), 1.59 (s, 3H, 4'- CH_3), 1.72 (brs, 3H, 5''- CH_3), 1.74 (brs, 3H, 4''- CH_3), 1.97 (s, 3H, OAc), 3.32 – 3.15 (m, 2H, 1'- CH_2), 4.80 – 4.65 (m, 2H, 1''- CH_2), 5.11 (dd, $J = 9.5, 7.7$ Hz, 1H, 2'-CH), 5.56 (t, $J = 7.2, 1.4$

Hz, 1H, 2''-CH), 6.20 (d, $J = 9.5$ Hz, 1H, 3-CH), 6.94 (brs, $J = 1.2$ Hz, 1H, 5-CH), 7.57 (d, $J = 9.5$ Hz, 1H, 4-CH).

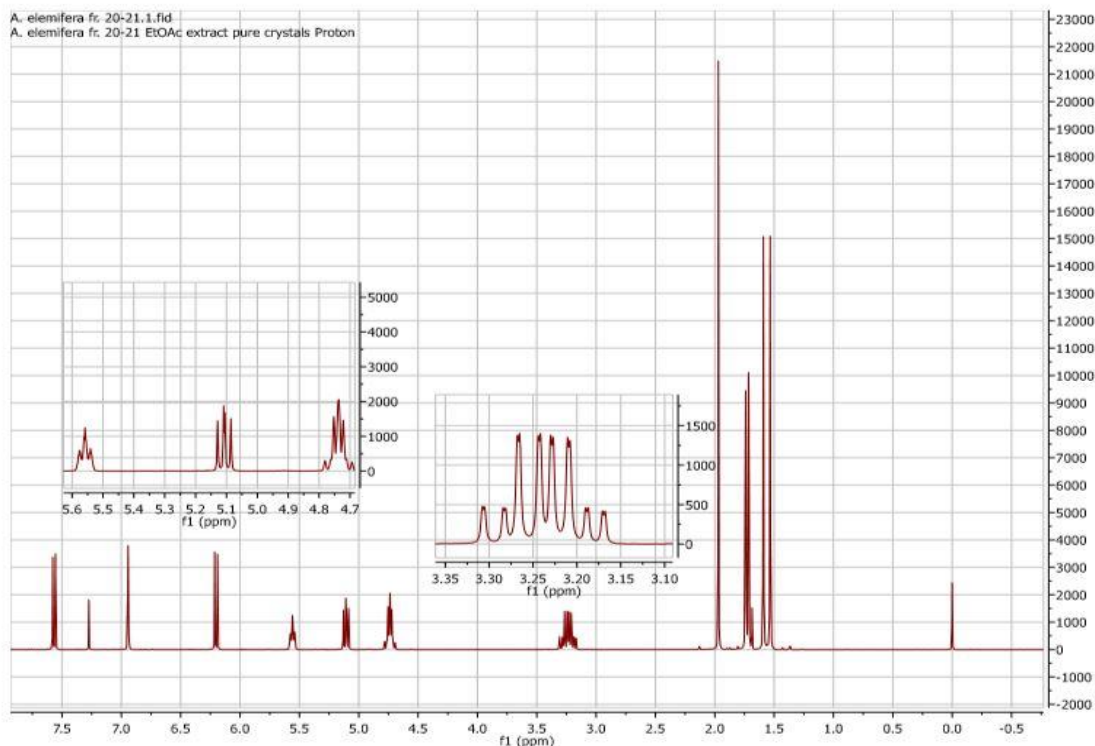


Figure 8. ^1H NMR spectrum of pure **1** crystals.

There were a few peaks in the ^1H NMR spectrum that were not clearly distinguished as a triplet, quartet, etc. like the one in the inset in the middle of **Figure 8**. Since there were those instances of unusual splitting patterns, the DQ COSY NMR spectrum (**Figure 9**) was analyzed to determine correlations between hydrogens that could explain the unusual spin-coupling occurrences. The DQ COSY spectrum depicts how hydrogens can interfere with one another's signals, which would be a plausible cause for the uncommon peak appearances. These hydrogen-hydrogen correlations can be visualized in **Figure 10**, which takes the information in **Figure 9** and illustrates how hydrogens in the actual

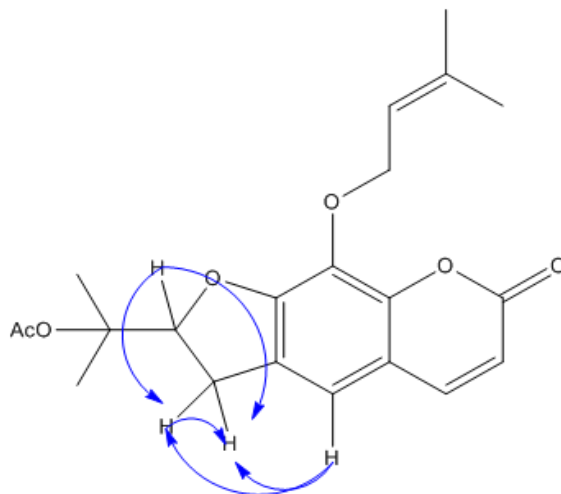


Figure 10. The COSY correlations concluded from the DQ COSY NMR spectrum of pure **1**.

Figure 10 shows that several hydrogens in close proximity with each other cause further splitting of the peaks, especially because the hydrogens on carbon 1' (**Figure 7**) are not exactly chemically equivalent and therefore have different J-coupling constants. Differences in J-coupling constants change the distance between the splits in signals, deviating the peak from a traditional triplet, doublet, etc. Therefore, instead of seeing the expected doublet from the two hydrogens on carbon 1' (**Figure 7**), that doublet is further split into a multiplet due to the correlations seen in **Figure 10**.

The structure of **2** was also confirmed using NMR and MS (**Appendix**) and is shown in **Figure 11**.

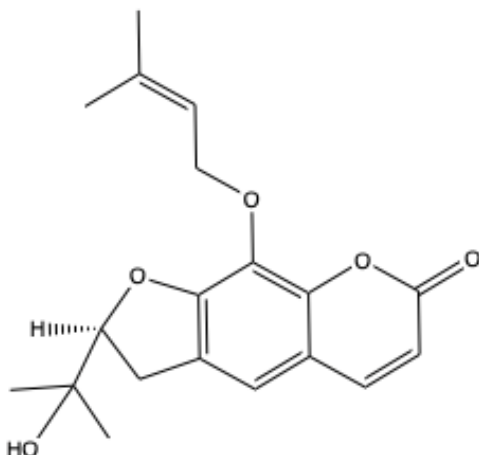


Figure 11. The determined structure of **2**, a previously isolated furanocoumarin and the hydroxy analog of **1**.

The NMR data for **2** had the same instances of unusual peak splitting as **1** and can be explained by the same correlations seen in **Figure 10**. The significant difference in the NMR spectra of **1** and **2** was the lack of a singlet from **1**'s extra methyl group (1.97 ppm in **Figure 8**) in the spectrum of **2**.

Quantification of **1** using HPLC produced the chromatogram in **Figure 12**, showing that **1** is the major constituent of the EtOAc extract. A series of serial dilutions of pure **1** with concentrations 1, 0.5, 0.25, 0.125, 0.0625, and 0.03125 mg/mL (using DCM as the solvent) were used to construct a calibration curve in order to quantify the amount of **1** per gram of crude EtOAc extract. The curve is included below, in **Figure 13**, and the area under the curve of **1** in **Figure 12a** (the large peak) was inserted into the equation in **Figure 13** to determine the

concentration of **1** in the crude extract. That calculation indicates that the concentration of **1** per gram of crude EtOAc extract is 351mg.

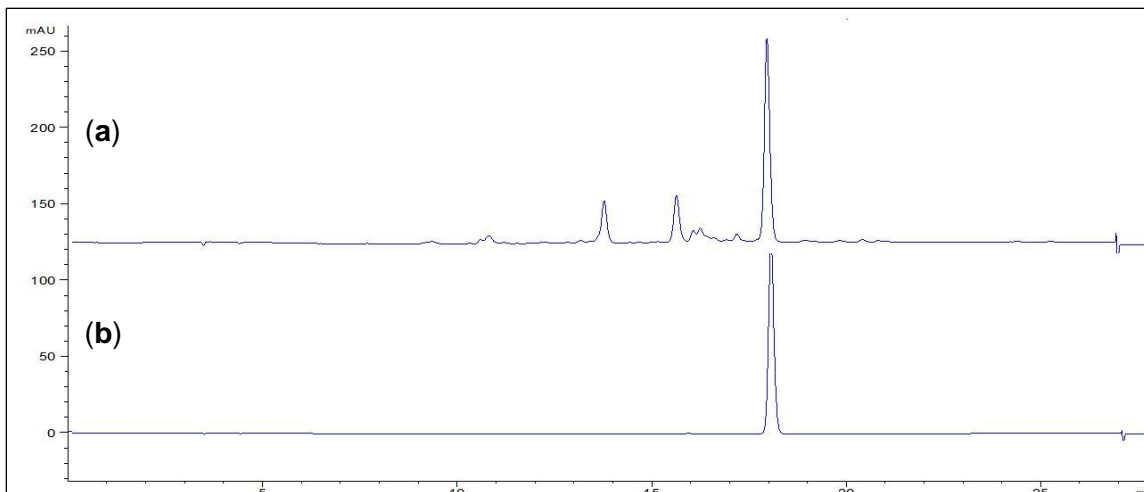


Figure 12. HPLC-generated chromatogram of the crude EtOAc extract (a) and pure **1** (b) at concentration 0.5mg/mL and detected at 254nm. Analysis was run with 5 μ L injection volume and 1.0mL/min flow rate.

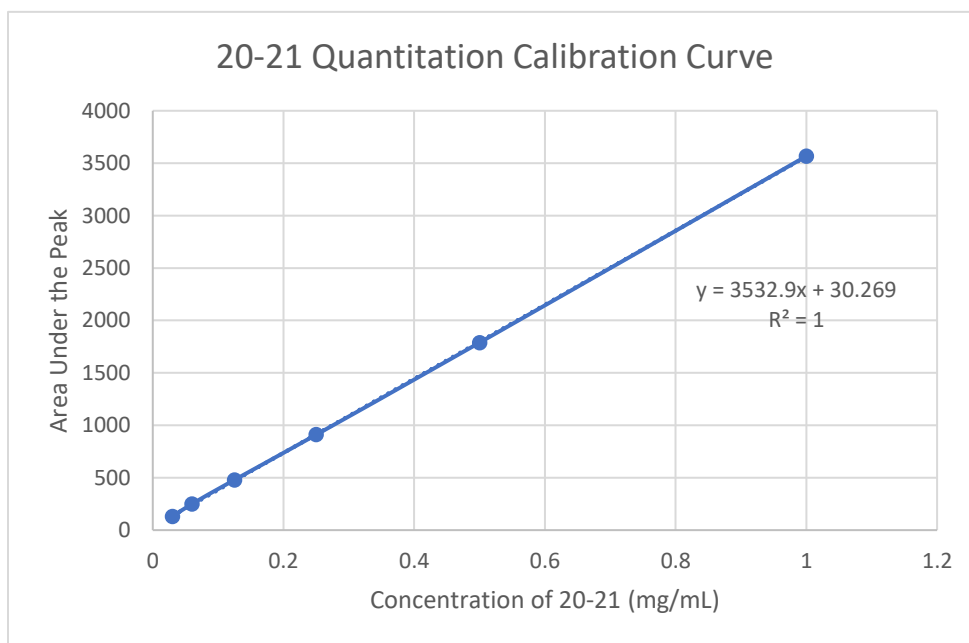


Figure 13. Calibration curve generated from serial dilutions of 20-21 at concentrations 1, 0.5, 0.25, 0.125, 0.0625, 0.03125 mg/mL. The area of the crude extract at 1mg/mL was plugged into the given equation as y in order to find x, the concentration of 20-21 per gram of crude EtOAc extract.

Results from the X-ray crystallography of **1** show that the absolute stereochemistry at the C-2' carbon of **1** is the S configuration (**Figure 14**). Stereochemistry refers to atoms' arrangement in space around a chiral carbon, or within a chiral molecule. Chiral carbons are those that are sp³ hybridized and have four different groups attached at each bonding site [18]. There is only one chiral carbon in **1** and **2**, C2' (**Figure 14**), and the stereochemistry of the carbon can influence the physical and chemical properties of the compound.

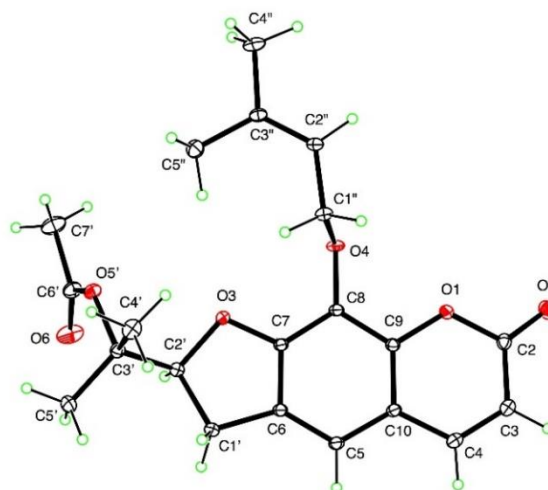


Figure 14. The crystal structure of **1** from the X-ray data, which shows that the absolute stereochemistry at the C-2' carbon is the S configuration.

Since the stereochemistry of the C-2' carbon is not changed during the base hydrolysis of **1**, the synthetic KOH product also has the absolute stereochemistry of S at that carbon, which has not been previously reported for **2**. Optical rotation measurements indicate that the KOH product from **1** and isolated, naturally occurring **2** have the same value at $[\alpha]_D (-)18.3$ ($c = 0.01$, CHCl_3). Furthermore, the NMR data for both the synthetic and natural **2** are in agreement, which further

proves the compounds are identical. Though the NMR data from **2** matches previously published findings, the initial reported optical rotation for the compound was $[\alpha]_D (+) 126$ ($c = 0.2$, CHCl_3), indicating the need for further investigation into the optical rotations of **2** ^[19]. The measured optical rotation for **1** was found to be $[\alpha]_D (-) 37.8$ ($c = 0.01$, CHCl_3). Further experiments outside of the scope of this investigation can be conducted to try to alter the stereochemistry of **1** to find its enantiomer, which would have the absolute configuration of R at carbon C2'.

II. Bioactivity of Isolated Compounds.

The initial phytotoxicity bioassay (**Table 1**) showed that the crude EtOAc extract of the leaves was slightly inhibitory towards both species of plant studied.

Table 1: Results of the Phytotoxicity Bioassay of *A. elemifera* leaves' EtOAc Extract

Sample ID	Tested Concentration	Solvent Used	Day	Lettuce	Agrostis
<i>A. elemifera</i> leaf (EtOAc extract)	1 mg/mL	10% acetone in DI H ₂ O	7	2	2

Table 1. The first phytotoxicity test results of the crude EtOAc extract. Rankings are based on a scale of 0-5, with 0 having no inhibitory effect and 5 having no seed germination.

Since the crude extract results showed promise, the investigation into the individual constituents continued. After isolation of **1** and **2**, the same phytotoxicity bioassay was performed on the pure compounds, yielding the results in **Table 2** below.

Table 2: Results of the Phytotoxicity Bioassay of Pure 1 and 2

Tested Concentration (μM)	Day	Lettuce (1)	Agrostis (1)	Lettuce (2)	Agrostis (2)
3	8	0	0	0	0
10	8	0	1	0	0
33	8	0	2	0	0
100	8	0	3	1	0
330	8	0	4	2	2
1000	8	2	4	2	2

Table 2. Results of the phytotoxicity bioassay of pure **1** and **2**. Rankings are based on a scale of 0-5, with 0 having no inhibitory effect and 5 having zero seed germination. Solvent used was 10% acetone in DI water.

Compound **1** showed more phytotoxicity than **2** in the case of the monocot *A. stolonifera* at concentrations of 10, 33, 100, 330, and 1000 μM , but in regard to *L. sativa*, **2** proved to be more inhibitory by a small margin at 100 and 330 μM .

A plausible explanation for the difference in phytotoxicity could be attributed to the slight increase in lipophilic character in **1** versus **2**, making it easier for **1** to enter the membrane of cells, disrupting normal growth of the plant. This also points to the mechanism of phytotoxicity of the two compounds being membrane related, which is corroborated in the cellular leakage test discussed later in this section.

The bioassay with *Lemna pausicostata* quantitatively describes the phytotoxicity of the compound tested by observing the effect of the compounds on leaves' number and coloration. Both **1** and **2** were tested at 30, 100, 300 and 1000 μM , and the results can be summarized in **Figures 15** and **16** below.

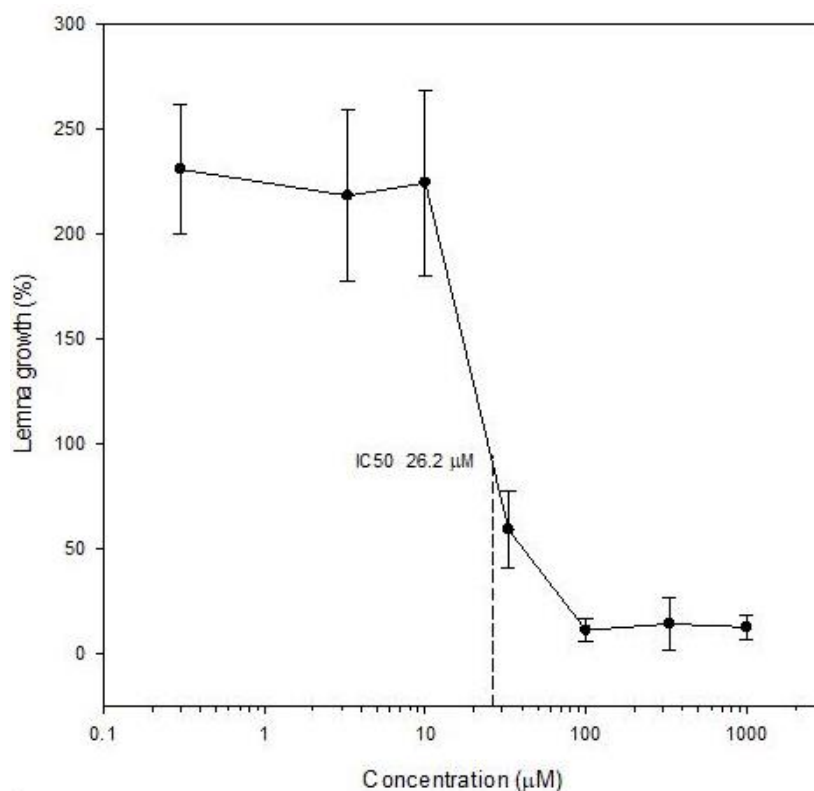


Figure 15. Results of the *L. pausicostata* assay for **1**, showing that its IC_{50} for the species is 26.2 μM . Error bars represent \pm one standard error of the mean.

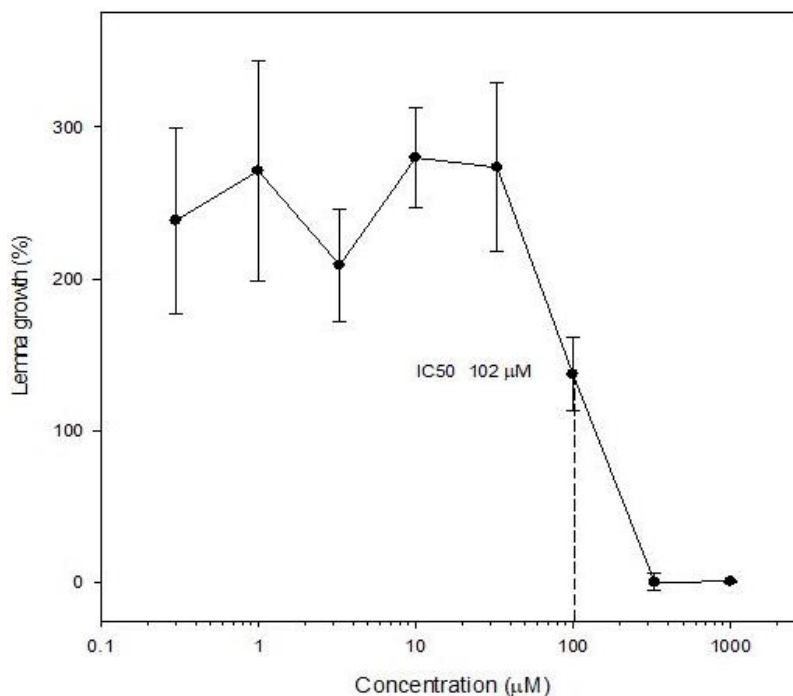


Figure 16. The *L. pausicostata* assay results for **2**, indicating that its IC₅₀ value is 102µM. Error bars represent +/- one standard error of the mean.

At all concentrations of **1** that were tested, inhibition occurred and bleaching of the leaves was observed (though no inhibition occurred at 10µM and below). Concentrations of **1** at 100µM and above caused total inhibition of growth, and the IC₅₀ value of **1** was shown to be 26.2µM (**Figure 15**). Comparatively, **2** was much less effective in its inhibition of plant growth (**Figure 16**), with no complete inhibition until a concentration of 330µM. The IC₅₀ value of **2** was much greater than **1** also, at 102µM, supporting the qualitative *L. sativa* and *A. stolonifera* phytotoxicity assay in the conclusion that **2** is not as successful as **1** at hindering plant growth. The exact mechanism of action of inhibition cannot be determined from this experiment, but since bleaching occurred in the leaves treated by **1**, it is likely that **1** interferes with either the synthesis of pigment or chloroplast

development in plant cells ^[20]. Due to the complicated structure of chloroplasts' inner membranes, and the impermeability of molecules through the thylakoid membrane, it is more likely that **1** interferes with the development of chloroplasts rather than the synthesis of chlorophyll—since the pigment is made within the thylakoid membrane ^[21]. As discussed earlier, there is a high probability that **1** interferes with cellular membrane function, and its structure could also induce obstruction of chloroplasts' outer membrane performance.

The cellular leakage test was run to determine if the phytotoxic activity of **1** was only membrane related, or if the process could be activated by light. If the phytotoxic method of action involves disruption of the membrane, then electrolytic cellular components would be released into the solution, increasing the conductivity of the solution. The results of the assay can be seen in **Figure 17**, showing different concentrations of **1** and the positive control, acifluorfen.

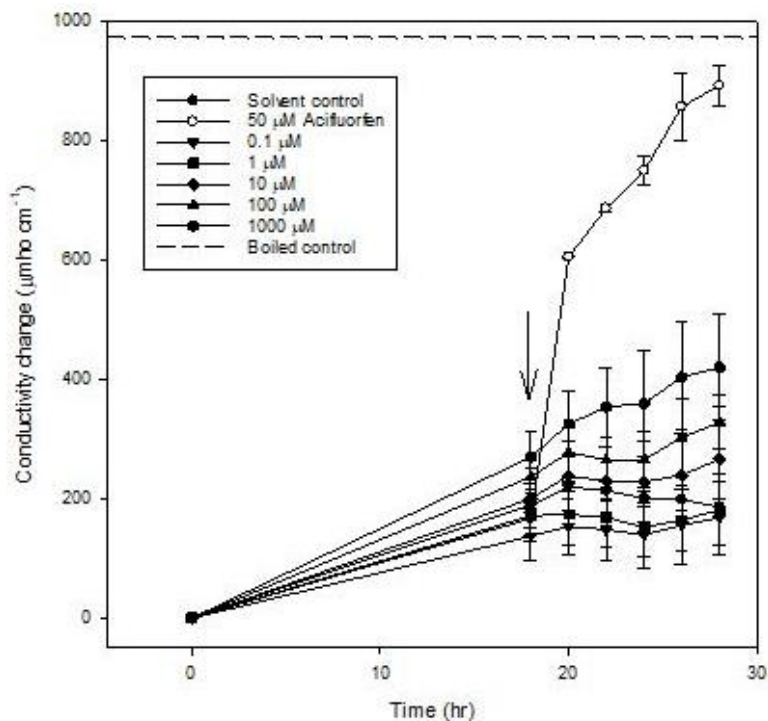


Figure 17. The cellular leakage test results showing conductivity of the solution after treating cucumber leaf disks with pure **1** at concentrations 1, 10, 100, and 1000 μM . Disks boiled in MES buffer represent the maximum possible conductivity (dotted line). The error bars represent +/- one standard error of the mean.

From **Figure 17**, it can be seen that **1** causes slight membrane leakage in the dark, and the extent of leakage relied upon the concentration of the compound. After exposure to light at 18 hours, there is little change in the leakage value—the most variation occurred in the 1000 μM dose—which indicates that the phytotoxicity mechanism is not light dependent. This is further corroborated by the positive control, acifluorfen, which is known to cause intense cellular leakage when exposed to light; since **1** does not produce leakage at all comparable to acifluorfen, the mechanism of **1** is most likely only membrane related. This result is slightly unusual because there is thorough research showing the tendency of

furanocoumarins, especially those deriving from psoralen, to have significant photosensitization [22]. The damage that psoralen derivatives cause once photoactivated is usually widespread across all important biological macromolecules (lipids, carbohydrates, nucleic acids, etc.), so it is unique that **1** seems to only disrupt lipids and does not require light to do so [22].

In the antifungal bioautography, **1** proved to have antifungal activity against *Colletotrichum* species. *Colletotrichum fragariae* is a cylindrical fungus that causes anthracnose crown rot (**Figure 18**) in crops such as strawberries, eventually resulting in the total death of the plant and severe economic loss [23].



Figure 18. Strawberry affected by anthracnose crown rot, evident from the necrotic tissue and red and white marbling. Taken from Reference #23 (permission pending): Louws, Frank, et al. “Anthracnose Crown Rot of Strawberry.” *NC State Extension Publications*, NC State, 2014, content.ces.ncsu.edu/anthracnose-crown-rot-of-strawberry.

In the assay, **1** showed inhibition in the growth of the fungus on the TLC plate, which is shown in **Figure 19** below.



Figure 19. A picture of the bioautography TLC plate, showing the antifungal activity of **1** (the white spot indicated by the arrow).

Though **1** did show antifungal activity, it only did so at a minimum concentration of 1000 μ M, indicating that the compound did not have strong enough activity to warrant further investigation into this property, or a determination of its IC₅₀. Additionally, **2** was studied in the same assay, but showed no fungicidal activity at any concentration. However, further investigation into other fungal species is warranted for **1**, since it could be more active and more useful against other agriculturally devastating fungi species. Several studies have been conducted on the antifungal activity of furanocoumarins, and they are known for strongly suppressing pathogenic fungi growth in the event of an attack (as furanocoumarins are released by plants for defense) [24]. Therefore, a more thorough experiment involving several other fungal species is warranted in order to truly determine the fungicidal properties of **1**.

III. Comparison of **1** to (S)-Limonene.

Both **1** and (S)-Limonene were submitted to the antibacterial bioassay to compare the new compound to the well-known bioactive limonene. The results of the antibacterial assays are summarized below, in **Table 3**.

Table 3: Results of the Antibacterial Bioassay for **1 and (S)-Limonene**

Species Tested	Initial Percent Inhibition (1)	Determined IC ₅₀ Value (1)	Initial Percent Inhibition (Limonene)	Determined IC ₅₀ Value (Limonene)
<i>Candida albicans</i>	60%	>20µg/mL	0	>20µg/mL
<i>Aspergillus fumigatus</i>	0	>20µg/mL	0	>20µg/mL
<i>Cryptococcus neformans</i>	0	>20µg/mL	0	>20µg/mL
MRSA	0	>20µg/mL	0	>20µg/mL
<i>E. coli</i>	0	>20µg/mL	0	>20µg/mL
<i>Pseudomonas aeruginosa</i>	0	>20µg/mL	0	>20µg/mL
<i>Klebsiella pneumoniae</i>	0	>20µg/mL	0	>20µg/mL
VRE	0	>20µg/mL	0	>20µg/mL

Table 3. The results of the antibacterial tests run on **1** and (S)-Limonene. Percent Inhibitions were determined qualitatively, and IC₅₀ values were not calculated due to the lack of inhibition of the tested concentration, 20µg/mL.

According to the data in **Table 3**, **1** only showed inhibition towards *Candida albicans*, a pathogenic yeast species. Though the percent inhibition was high enough to warrant investigation into the IC₅₀ value for **1**, there was no further inhibition at concentrations lower than 20µg/mL, meaning that **1** did not have enough of an effect to be seriously considered as an antibacterial agent. Though there was no effect on the other species in the first assay, the IC₅₀ value exists,

and is known to be at least $>20\mu\text{g/mL}$. Similarly, since (S)-Limonene showed no activity at all, its IC_{50} values for each species are just assumed to be $>20\mu\text{g/mL}$, also indicating that compound would not be a satisfactory antibacterial agent against the tested species. This result is not what was expected, considering the studied effect of limonene on other bacterial species [25,26]. It is possible that limonene is active against species that were not tested in this investigation, and that it may have an effect at higher concentrations than were measured—though that would indicate it is still a poor contender for agricultural use. A more thorough, wider scope comparison should be pursued between the two compounds to truly determine the benefit of one over the other regarding antibacterial activity.

Results from the antifungal assay of limonene show that the compound has no significant inhibition towards the growth of *Colletotrichum fragariae* (**Figure 20**). This result was also unexpected, since limonene has been proven to be significantly antifungal towards several species [6,27]. However, a wider investigation with other agriculturally significant species should be conducted for both compounds to more thoroughly compare their antifungal activity.



Figure 20. A picture of the bioautography TLC plate with (S)-Limonene. There is no obvious antifungal activity present on the plate.

The purpose of the comparison between **1** and (S)-Limonene was to study the difference in biological properties between the major component of the EtOAc extract of the leaves (which can also be assumed to be one of the dominant compounds in the leaves in general) and the major component of the essential oil of the plant. Though most plant essential oils have not been subjected to scrutinized investigations, there is evidence that many plants' oils (acquired through steam distillation of the leaves) have varying bioactivity [28]. There are several studies that show a diverse selection of essential oils' aptitude for insecticidal, fungicidal, and phytotoxic activity [28]. Furthermore, several experiments have shown that a wide spectrum of essential oils have significant antimicrobial properties [29]. This plethora of bioactivity can possibly be attributed to the complex mixture of compounds usually present in the essential oils. Steam distillation dominates the methods for essential oil extraction (93% of all

extraction is done by steam distillation), but it is a complicated process that requires specialized equipment and does not consistently produce significant yields [30]. The liquid-liquid extraction method used to isolate **1** is a much simpler process, so if **1** had shown greater success than (S)-Limonene in the bioassays, then steam distillation of *Amyris elemifera*'s essential oil would not be necessary—because **1** would have been more agriculturally beneficial than the essential oil. This also assumes that, since (S)-Limonene is the major component of the essential oil (45%), it accounts for the oil's bioactivity; there are likely compounds in the oil that have higher specific activity than both (S)-Limonene and **1**, but there may not be a significant enough amount to explore those other constituents. However, since there were no truly conclusive results in the comparison of the two compounds (most likely attributed to the limited selection of plant, fungal, and microbial species used), further investigation into the benefit of the essential oil over the novel furanocoumarin is justified.

Conclusion.

A novel furanocoumarin (**1**) was isolated using fractionation methods from the EtOAc extract of the leaves of *Amyris elemifera*, a plant in the family Rutaceae that is well-known for its bioactive properties. After NMR and MS analysis of the pure **1**, its structure was determined, at which point its status as a newly discovered compound was confirmed. This investigation was therefore the first to report the bioactivity of **1**, which was determined to be the major constituent of the EtOAc extract at 351mg of it per gram of extract. Through several experiments, it was concluded that **1** showed both antifungal and phytotoxic activity against *Colletotrichum fragariae* (fungus) and the plants *Lactuca sativa*, *Agrostis stolonifera*, and *Lemna paucicostata*; the IC₅₀ value of phytotoxicity was determined for the latter and was found to be 26.2µM. The mechanism of phytotoxic action was indicated as membrane related, not light dependent, based upon a cellular leakage assay. However, the exact mechanism is still unknown and requires further investigation to understand. A comparison between **1** and (S)-Limonene, the major constituent of the plant's essential oil, was done with an antibacterial and antifungal assay, since there have been previous investigations into the effects of limonene. This comparison yielded unexpected results, where there was little activity shown by both

compounds in the antibacterial assay, and significantly greater antifungal activity by the novel furanocoumarin.

Another constituent (**2**) was also isolated from the EtOAc extract, but NMR and MS data showed it was identical to a previously studied compound. This compound was also submitted to the antifungal and phytotoxic assays, but it showed no significant activity.

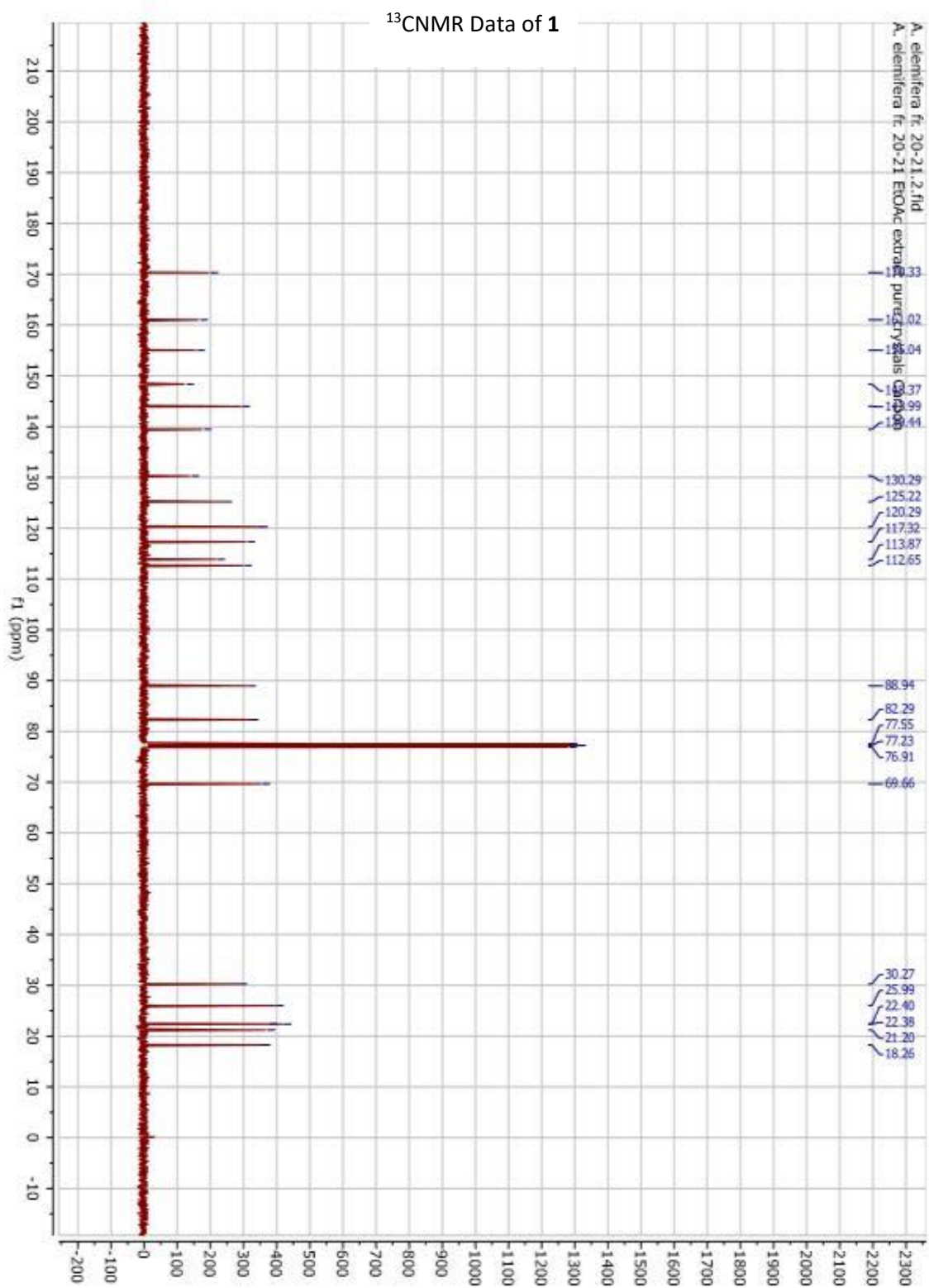
List of References

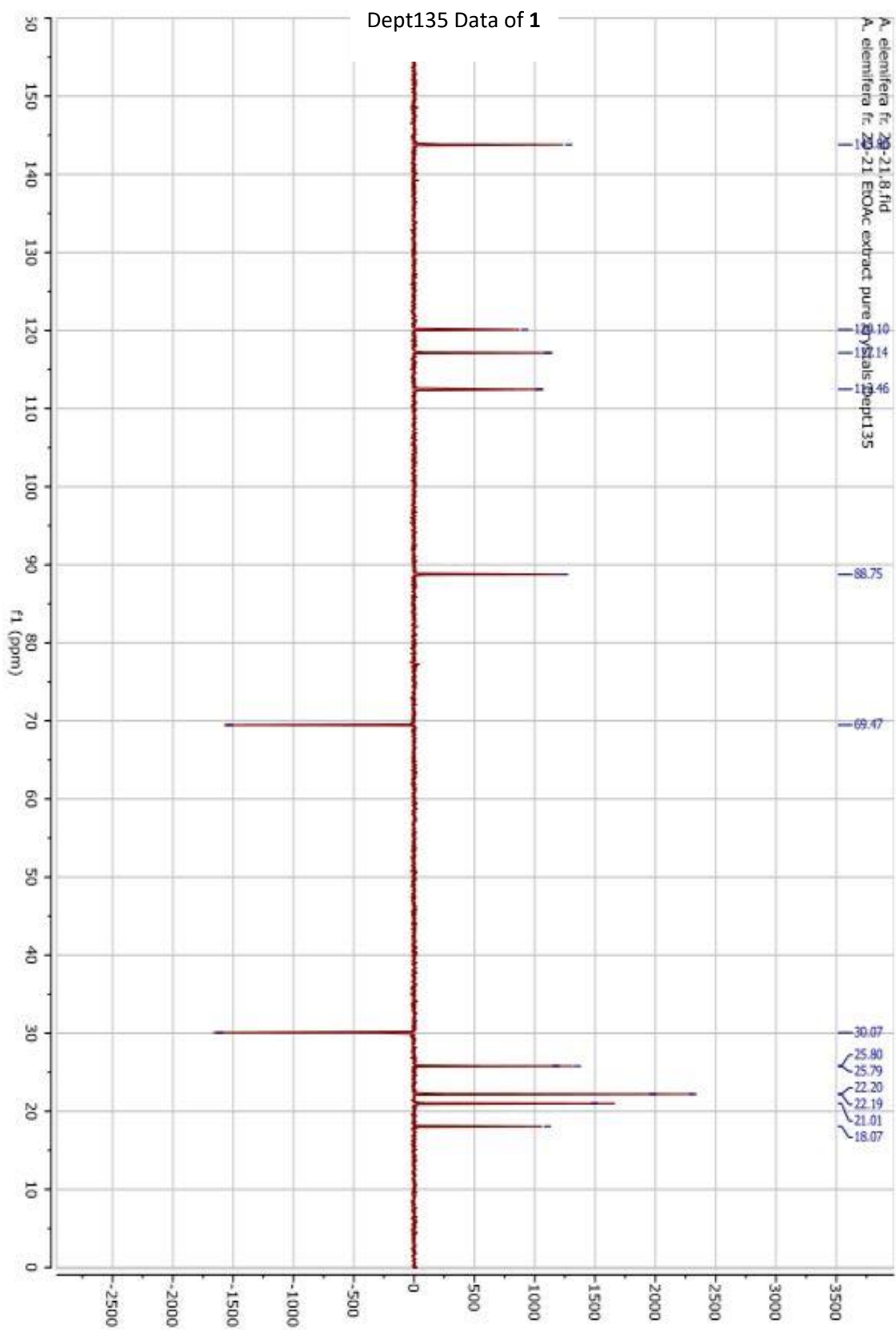
1. Dayan, Franck E., et al. "Natural Products in Crop Protection." *Bioorganic & Medicinal Chemistry*, vol. 17, no. 12, 2009, pp. 4022–4034., doi:10.1016/j.bmc.2009.01.046.
2. Macías, Francisco A., et al. "Search for a Standard Phytotoxic Bioassay for Allelochemicals. Selection of Standard Target Species†." *Journal of Agricultural and Food Chemistry*, vol. 48, no. 6, 2000, pp. 2512–2521., doi:10.1021/jf9903051.
3. "Chapter 24: Natural Products (Secondary Metabolites)." *Biochemistry & Molecular Biology of Plants*, by Bob B. Buchanan et al., I.K. International, 2000, pp. 1250–1318.
4. Nebo, Liliane, et al. "Phytotoxicity of Alkaloids, Coumarins and Flavonoids Isolated from 11 Species Belonging to the Rutaceae and Meliaceae Families." *Phytochemistry Letters*, vol. 8, 2014, pp. 226–232., doi:10.1016/j.phytol.2014.02.010.
5. Setzer, William N, et al. "Leaf Oil Compositions and Bioactivities of Abaco Bush Medicines." *PharmacologyOnLine*, vol. 3, 2006, pp. 794–802., pharmacologyonline.silae.it/files/archives/2006/vol3/093.Setzer.pdf.
6. Marei, Gehan I.kh., et al. "Comparative Antifungal Activities and Biochemical Effects of Monoterpenes on Plant Pathogenic Fungi." *Pesticide Biochemistry and Physiology*, vol. 103, no. 1, 2012, pp. 56–61., doi:10.1016/j.pestbp.2012.03.004.
7. Sun, Jidong. "D-Limonene: Safety and Clinical Applications." *Alternative Medicine Review*, vol. 12, no. 3, 2007, pp. 259–264.
8. Jing, Li, et al. "Antifungal Activity of Citrus Essential Oils." *Journal of Agricultural and Food Chemistry*, vol. 62, no. 14, 2014, pp. 3011–3033., doi:10.1021/jf5006148.
9. Kohli, Pooja, et al. "Pectin Methylesterases: A Review." *Journal of Bioprocessing & Biotechniques*, vol. 05, no. 05, 2015, doi:10.4172/2155-9821.1000227.
10. Salas-Tovar, Jesús A., et al. "Analytical Methods for Pectin Methylesterase Activity Determination: A Review." *Food Analytical Methods*, vol. 10, no. 11, 2017, pp. 3634–3646., doi:10.1007/s12161-017-0934-y.

11. Lionetti, Vincenzo, et al. "Three Pectin Methyltransferase Inhibitors Protect Cell Wall Integrity for Arabidopsis Immunity to Botrytis." *Plant Physiology*, vol. 173, no. 3, 2017, pp. 1844–1863., doi:10.1104/pp.16.01185.
12. Scott, Barry R., et al. "Molecular and Genetic Basis of Furocoumarin Reactions." *Mutation Research/Reviews in Genetic Toxicology*, vol. 39, no. 1, 1976, pp. 29–74., doi:10.1016/0165-1110(76)90012-9.
13. Raina-Fulton, Renata, and Aisha Mohamad. "Pressurized Solvent Extraction with Ethyl Acetate and Liquid Chromatography—Tandem Mass Spectrometry for the Analysis of Selected Conazole Fungicides in Matcha." *Toxics*, vol. 6, no. 4, 2018, p. 64., doi:10.3390/toxics6040064.
14. Dayan, Franck E, et al. "Investigating the Mode of Action of Natural Phytotoxins." *Journal of Chemical Ecology*, vol. 26, no. 9, 2000, pp. 2079–2094.
15. Haffner, Oto, et al. "Application of Information Technologies For Visual Evaluation of Lemna Minor Bioassays." *International Journal Information Technology Applications*, vol. 7, no. 1, July 2018, pp. 85–97.
16. Duke, Stephen O, and William H Kenyon. "Peroxidizing Activity Determined by Cellular Leakage." *Target Assays for Modern Herbicides and Related Phytotoxic Compounds*, by Böger Peter and Gerhard Sandmann, Lewis Publishers, 1993, pp. 61–66.
17. Wedge, D. E., & Kuhajek, J. M. (1998). A microbioassay for fungicide discovery. *SAAS Bulletin of Biochemistry and Biotechnology*, 11, 1-7.
18. "Identifying Chirality Centers (Video)." *Khan Academy*, Khan Academy, www.khanacademy.org/science/organic-chemistry/stereochemistry-topic/chirality-r-s-system/v/chirality-center-jay.
19. Hasan, Choudhury M., et al. "Chemical Similarities between Microcybe Multiflora Turcz, and the Rutaceous Genus Phebalium." *Biochemical Systematics and Ecology*, vol. 21, no. 5, 1993, pp. 625–627., doi:10.1016/0305-1978(93)90064-x.
20. Mayonado, David J., et al. "Evaluation of the Mechanism of Action of the Bleaching Herbicide SC-0051 by HPLC Analysis." *Pesticide Biochemistry and Physiology*, vol. 35, no. 2, 1989, pp. 138–145., doi:10.1016/0048-3575(89)90111-9.
21. Cooper GM. *The Cell: A Molecular Approach*. 2nd edition. Sunderland (MA): Sinauer Associates; 2000. Chloroplasts and Other Plastids. Available from: <https://www.ncbi.nlm.nih.gov/books/NBK9905/>

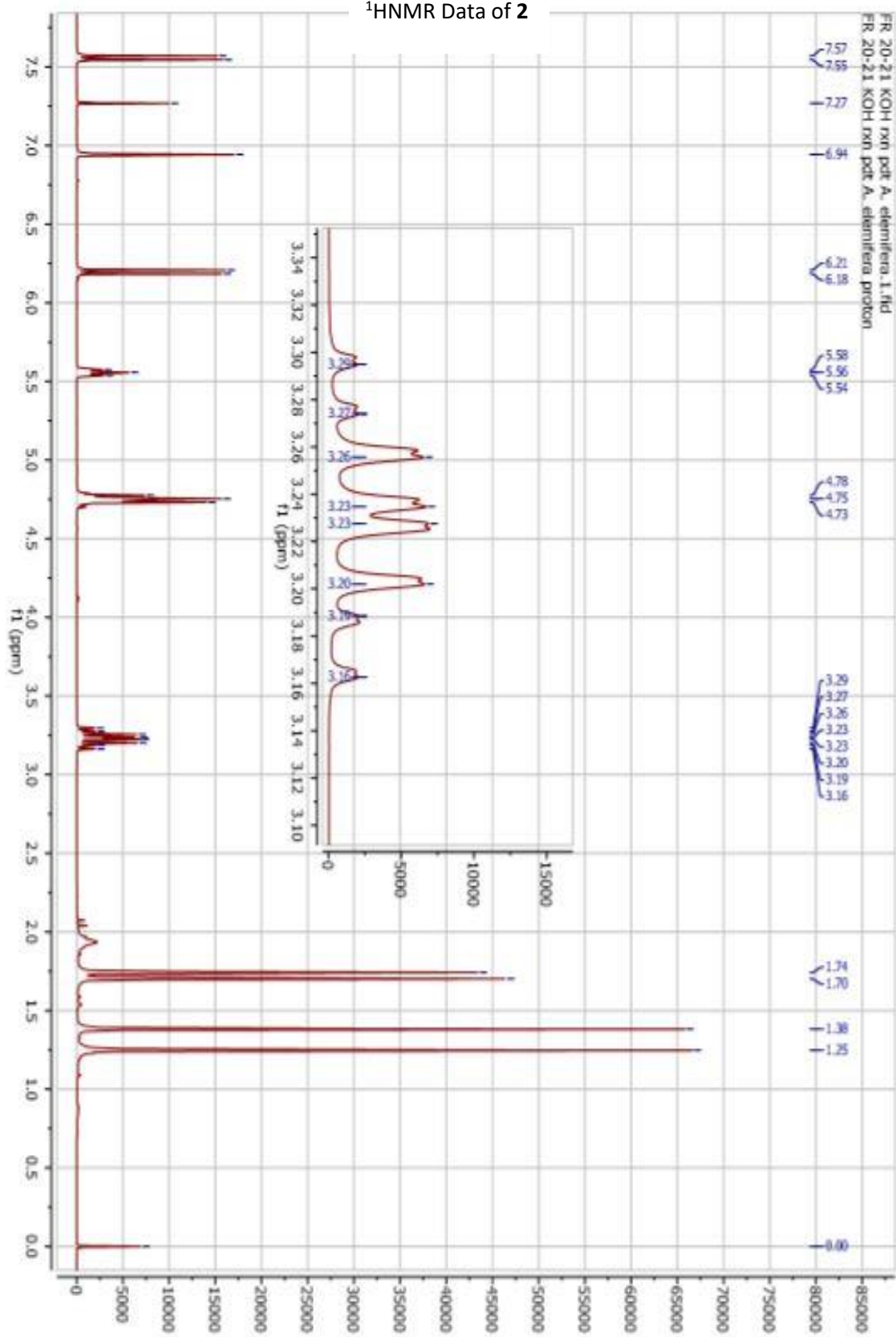
22. Bruni, Renato, et al. "Botanical Sources, Chemistry, Analysis, and Biological Activity of Furanocoumarins of Pharmaceutical Interest." *Molecules*, 2019, doi:10.3390/molecules24112163.
23. Louws, Frank, et al. "Anthracnose Crown Rot of Strawberry." *NC State Extension Publications*, NC State, 2014, content.ces.ncsu.edu/anthracnose-crown-rot-of-strawberry.
24. Razavi, Seyed Mehdi. "Plant Coumarins as Allelopathic Agents." *International Journal of Biological Chemistry*, vol. 5, no. 1, 2011, pp. 86–90., doi:10.3923/ijbc.2011.86.90.
25. Kim, Jeongmok, et al. "Antibacterial Activity of Some Essential Oil Components against Five Foodborne Pathogens." *Journal of Agricultural and Food Chemistry*, vol. 43, no. 11, 1995, pp. 2839–2845., doi:10.1021/jf00059a013.
26. Dorman, H. J. D., and S. G. Deans. "Antimicrobial Agents from Plants: Antibacterial Activity of Plant Volatile Oils." *Journal of Applied Microbiology*, vol. 88, no. 2, 2000, pp. 308–316., doi:10.1046/j.1365-2672.2000.00969.x.
27. Chee, Youn, et al. "In Vitro Antifungal Activity of Limonene against *Trichophyton Rubrum*." *Mycobiology*, vol. 37, no. 3, 2009, p. 243., doi:10.4489/myco.2009.37.3.243.
28. Isman, Murray B. "Plant Essential Oils for Pest and Disease Management." *Crop Protection*, vol. 19, no. 8-10, 2000, pp. 603–608., doi:10.1016/s0261-2194(00)00079-x.
29. Deans, S.g., and G. Ritchie. "Antibacterial Properties of Plant Essential Oils." *International Journal of Food Microbiology*, vol. 5, no. 2, 1987, pp. 165–180., doi:10.1016/0168-1605(87)90034-1.
30. Masango, Phineas. "Cleaner Production of Essential Oils by Steam Distillation." *Journal of Cleaner Production*, vol. 13, no. 8, 2005, pp. 833–839., doi:10.1016/j.jclepro.2004.02.039.

Appendix.

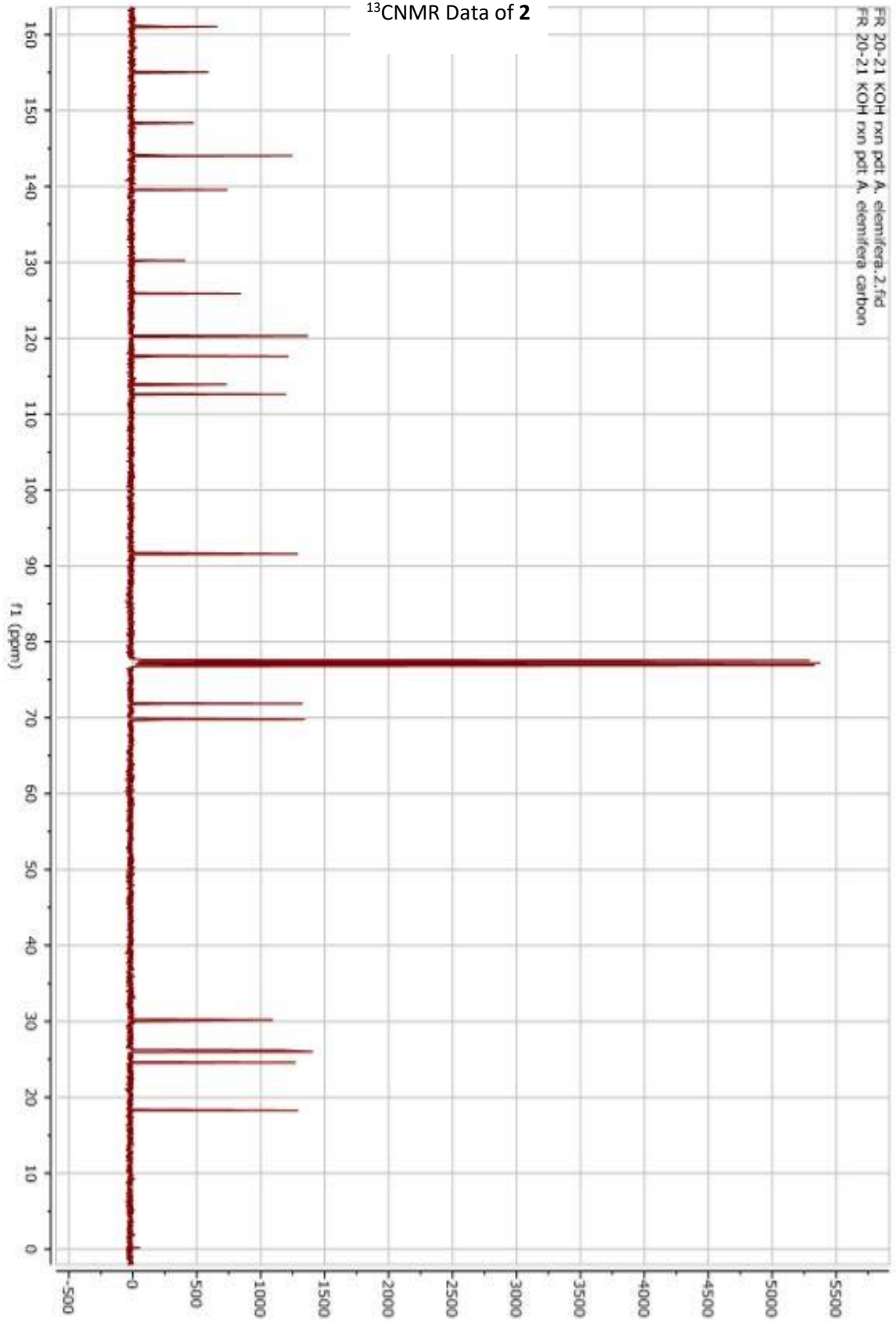


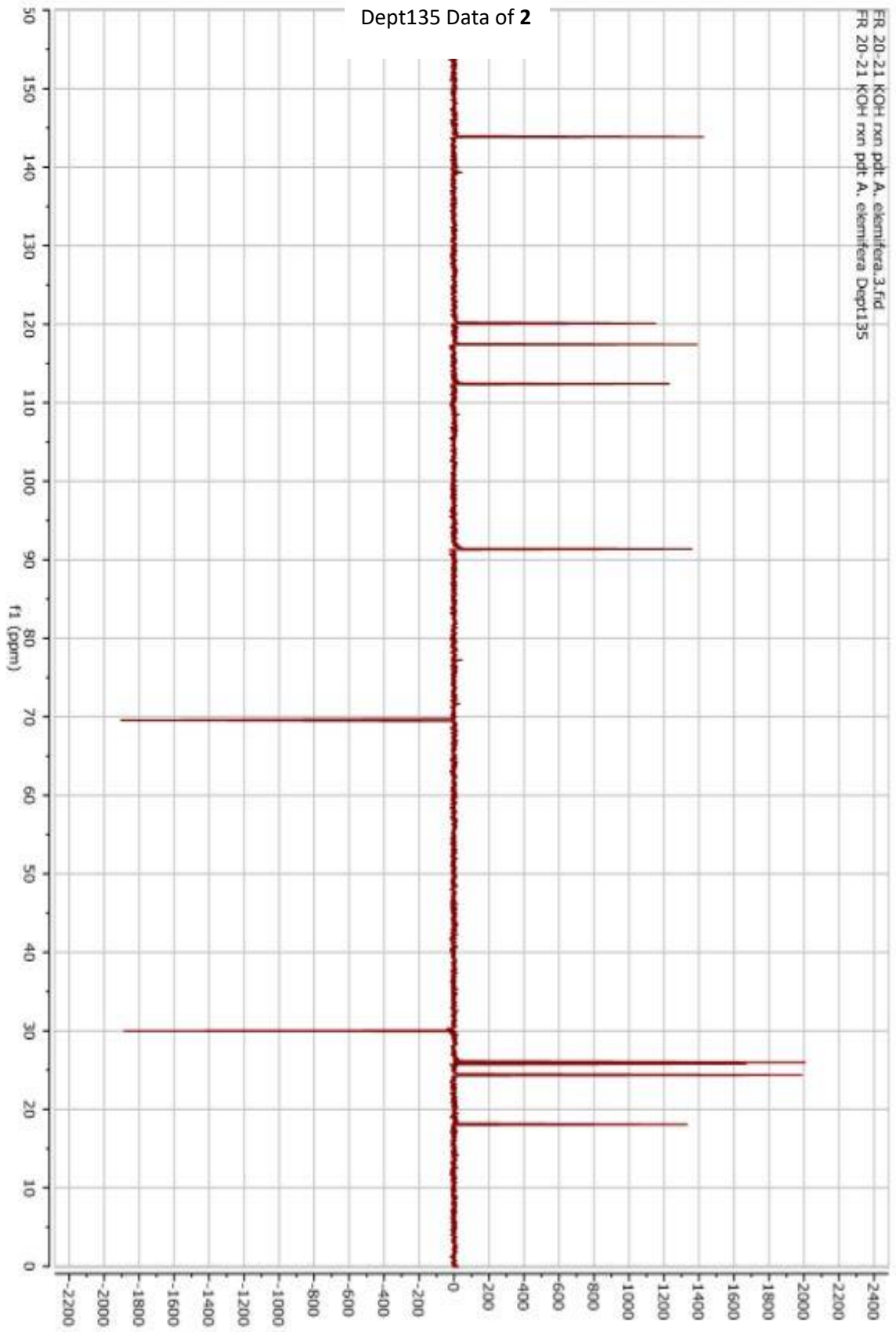


¹HNMR Data of 2

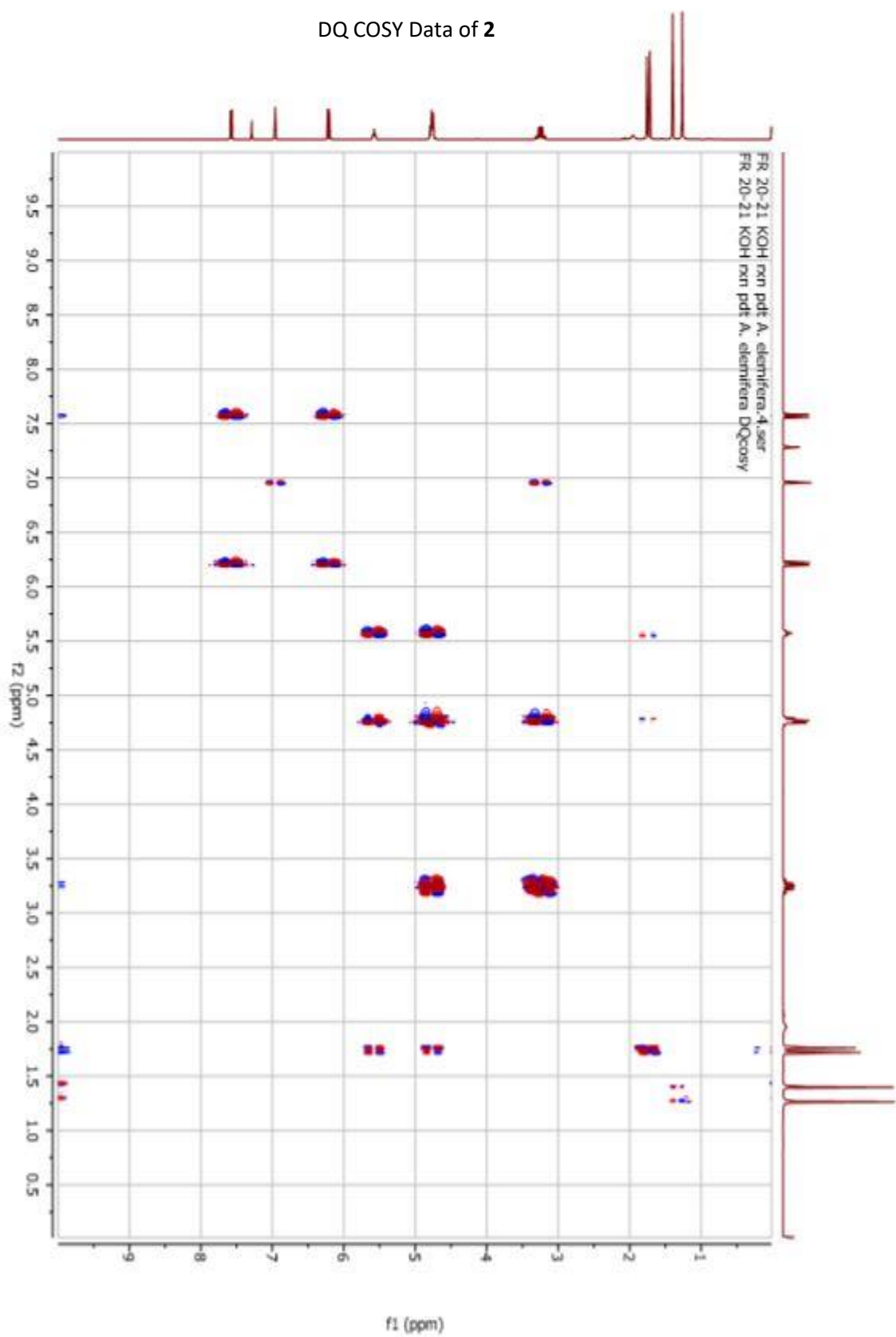


¹³CNMR Data of 2

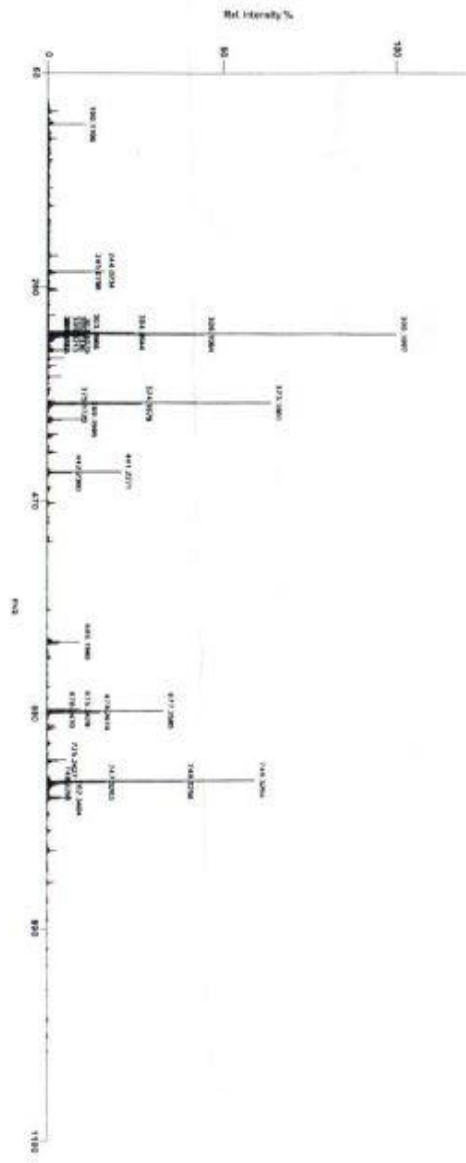




DQ COSY Data of 2



MS Data of 1



Elemental Compositions

Element Limits: C 0/50 H 0/91 O 0/10 N 0/10

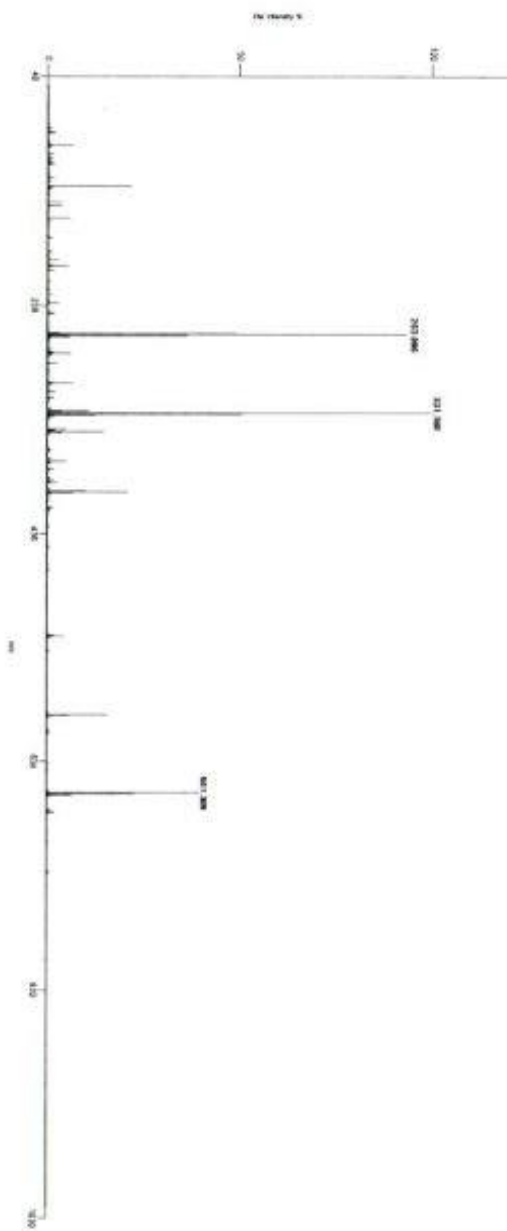
Tolerance: 5 mmu Even or odd electron ion or both: Even

Electron correction: None, Charges: 1

Minimum unsaturation: -1 Maximum unsaturation: 100

Calc. m/z	Abund %	mmu	Peaks	Score	DBE	Composition	NIST
373.166450	3.41	0.36	4	0.030283	14.5	C22H21O2N4	0
373.165114	3.89	0.53	4	0.051594	9.5	C21H25O6	0
373.163763	3.87	1.27	4	0.122809	15.5	C18H17N10	0
373.170473	2.46	2.50	4	0.153456	18.5	C27H21N2	0

MS Data of 2



Elemental Compositions

Element Limits: C 0/50 H 0/100 O 0/10

Tolerance: 5.0 mmu Even or odd electron ion or both: Both

Electron correction: None. Charges: 1

Minimum unsaturation: -1 Maximum unsaturation: 100

Calc. m/z	Abund %	mmu	DBE	Composition
331.154549	100.000	-0.33	8.5	C19H23O5